Cerebrospinal Fluid Flow in the Normal and Hydrocephalic Human Brain

Andreas A. Linninger*, Michalis Xenos, David C. Zhu, MahadevaBharath R. Somayaji, Srinivasa Kondapalli, and Richard D. Penn

***Abstract*—Advances in magnetic resonance (MR) imaging techniques enable the accurate measurements of cerebrospinal fluid (CSF) flow in the human brain. In addition, image reconstruction tools facilitate the collection of patient-specific brain geometry data such as the exact dimensions of the ventricular and subarachnoidal spaces (SAS) as well as the computer-aided reconstruction of the CSF-filled spaces. The solution of the conservation of CSF mass and momentum balances over a finite computational mesh obtained from the MR images predict the patients' CSF flow and pressure field. Advanced image reconstruction tools used in conjunction with first principles of fluid mechanics allow an accurate verification of the CSF flow patters for individual patients. This paper presents a detailed analysis of pulsatile CSF flow and pressure dynamics in a normal and hydrocephalic patient. Experimental CSF flow measurements and computational results of flow and pressure fields in the ventricular system, the SAS and brain parenchyma are presented. The pulsating CSF motion is explored in normal and pathological conditions of communicating hydrocephalus. This paper predicts small transmantle pressure differences between lateral ventricles and SASs ($\sim$ 10 Pa). The transmantle pressure between ventricles and SAS remains small even in the hydrocephalic patient ($\sim$ 30 Pa), but the ICP pulsatility increases by a factor of four. The computational fluid dynamics (CFD) results of the predicted CSF flow velocities are in good agreement with Cine MRI measurements. Differences between the predicted and observed CSF flow velocities in the prepontine area point towards complex brain-CSF interactions. The paper presents the complete computational model to predict the pulsatile CSF flow in the cranial cavity.**

***Index Terms*—Cerebrospinal fluid, computational fluid dynamics, human brain, hydrocephalus, intracranial pressure, reconstruction tools.**

I. Introduction

THE central nervous system composed of the brain and the spinal cord is submerged in cerebrospinal fluid (CSF). CSF, a colorless liquid with the consistency of blood plasma, is also found in four cavities inside the brain known as the ventricles, which in turn are connected to the cerebral and the spinal subarachnoidal spaces (SAS). The CSF surrounding the brain and the spinal cord is not at rest, but undergoes complex pulsating fluid motion in synchronization with the heartbeat. Advances in magnetic resonance imaging (MRI) have made possible accurate determination of CSF flow patterns *in vivo* [1]–[3]. Recently, on-line dynamic *in vivo* intracranial pressure (ICP) measurements have become available [4]. Despite of this progress in observing the CSF flows and pressures, the CSF flow dynamics in the normal brain and communicating hydrocephalus have not been accurately accounted for by the fundamental principles of fluid mechanics [5].

Various causes have been hypothesized to produce hydrocephalus. Early work suggested that large ICP differences between the ventricles and the SAS are responsible for the development of hydrocephalus [6]. More recent studies show in communicating hydrocephalus large transmantle pressure differences are not present [4], [7]. These clinical observations were explained by dynamic first principles methods [8]. The difficulty in accounting for intracranial dynamics is partially due to the structural and geometric complexity of the human brain which encompasses porous parenchymal brain tissue as well as fluid filled compartments (ventricles, SAS, and blood vessels). Several recent CSF flow studies to explain CSF flow patterns use one-dimensional models [9]–[11]. More realistic flow field simulations have been limited to small sections in the brain like the aqueduct of Sylvius [12], [13]. Other CSF flow models only considered compartmental models [14]. A rigorous quantification of the multidimensional CSF flow field based on basic fluid physics has not yet been achieved.

The lack of quantitative understanding of intracranial dynamics hampers the development of better treatment options for hydrocephalus. For the last thirty years, treatment relies on the placement of a shunt system that removes excess CSF from the cranial vault. Unfortunately, shunting has a high failure rate and multiple painful and expensive revision operations are required [15], [16]. Changes to ICP and CSF flow patterns in the hydrocephalic brain due to shunting are still poorly understood. The goal of our work is to elucidate the normal and hydrocephalic CSF flow patterns using rigorous fluid mechanical principles, and use these findings to improve the treatment of hydrocephalus.

The computational analysis presented in this paper integrates Cine MRI phase contrast imaging with accurate reconstruction of individual patients' brain geometry of their ventricular and the SASs. Experimental results include accurate measurements

Manuscript received January 25, 2006; revised June 24, 2006. This work was supported in part by the Sussman and Asher Foundation. *Asterisk indicates corresponding author.*

*A. A. Linninger is with the Laboratory for Product and Process Design (LPPD), Department of Chemical and Bioengineering, University of Illinois at Chicago, CEB 216, 851 S. Morgan St, Room 218 SEO, Chicago, IL 60607 USA (e-mail: linninge@uic.edu).

M. Xenos, M. R. Somayaji, and S. Kondapalli are with the Laboratory for Product and Process Design (LPPD), Department of Chemical and Bioengineering, University of Illinois at Chicago, Chicago, IL 60607 USA.

D. C. Zhu is with the Cognitive Imaging Research Center, Michigan State University, East Lansing, MI 48824 USA.

R. D. Penn is with the Departments of Surgery, University of Chicago, Chicago, IL 60637 USA.

Color versions of Figs. 9 and 10 are available online at http://ieeexplore.ieee.org.

Digital Object Identifier 10.1109/TBME.2006.886853

of the flow velocities and flow patterns in normal and in hydrocephalic subjects. In a detailed comparison, the CSF dynamics of one normal subject will be contrasted with the abnormal flow and pressure dynamics in a patient with communicating hydrocephalus. Rigorous fluid physics principles are used to quantify the flow and pressure fields defined in the computational grids reconstructed from the MR images for each subject. The computational approach will be shown to accurately quantify the changes in the ICP patterns for normal and hydrocephalic subjects.

Section II introduces the methods for measuring the CSF flow fields *in vivo*. It demonstrates the use of image reconstruction tools for generating accurate computational meshes of the patients' specific brain geometry and as an accurate framework for computational analysis of the measured CSF flow patterns. Section III will introduce the computational fluid dynamics (CFD) analysis for the entire brain and present results of the flow and pressure patterns of the normal and hydrocephalic case. This comprehensive model of the entire ventricular system is a first of its kind.

II. Methodology

Our aim is to use the physical principles of fluid flow to quantify intracranial CSF dynamics. The rigorous fluid mechanics approach proceeds in three stages. In step 1, MRI techniques are used to accurately measure the patients' individual brain geometry and the CSF flow velocities in select regions of interest. In step 2, *image reconstruction* is used to obtain the dimensions of the CSF pathways and the brain. It also converts the patient-specific MR data into accurate two or three-dimensional (3-D) surfaces and volumes. *Grid generation* is then used to partition these spaces into a large number of small finite volumes. CFD in step 3 solves the equations of fluid motion numerically over the discretized brain geometry. The agreement of the experimental MRI flow field with the CFD predictions demonstrates that the detailed mechanistic picture of fluid flows and pressures that cause intracranial dynamics is correct. Before presenting the intracranial dynamics in normal and hydrocephalic patients, the next subsection briefly introduces the experimental method as well as the mathematical background for this paper.

A. In Vivo CSF Flow Measurement

CSF flow velocity images at different time frames of the cardiac cycle are collected using two-dimensional (2-D) Cine phase-contrast techniques [17], [18] from 11 subjects (eight normal and three with hydrocephalus) on a 3T GE Signa scanner (GE Medical Systems, Milwaukee, WI). Velocity images in all three directions in 16 equidistant time frames of the cardiac cycle are collected at the mid-sagittal slice to view the major CSF pathways. The velocity images perpendicular to the slice of interest are collected to measure the CSF flow at 32 equidistant time frames of the cardiac cycle at a mid-coronal slice of the third ventricle, and then at an axial slice across the junction between the aqueduct of Sylvius and the fourth ventricle. The CSF pathway is segmented for analysis based on a T_2-weighted image, in which CSF was enhanced. The velocity of every pixel in these regions of CSF is calculated. Corrections are made for spatially dependent offset velocity due to eddy currents or head motion [1], [18], [19]. T_1-weighted volumetric axial or sagittal images (with CSF signal suppressed) are also collected to estimate the volumes of the different CSF pathway sections. Each volume (18 cm $\times$ 24 cm $\times$ 24 cm) of images contains 120 contiguous slices with a 1.5–mm thickness, a 24-cm field-of-view and a 256 $\times$ 256 reconstructed matrix size. The data acquisition and velocity calculation has been fully discussed in the paper by Zhu *et al.* [20]. Fig. 1 displays the results of MRI experiments: the flow of blood in the basilar artery (ml/min), the lateral ventricle area deformation (mm^2), the CSF flow at the third ventricle and at the junction of the aqueduct of Sylvius and the fourth ventricle (ml/min). Fig. 3 and Table IV summarize the CSF flow measurements of the patients at six locations of interest obtained with this Cine phase contrast imaging technique.

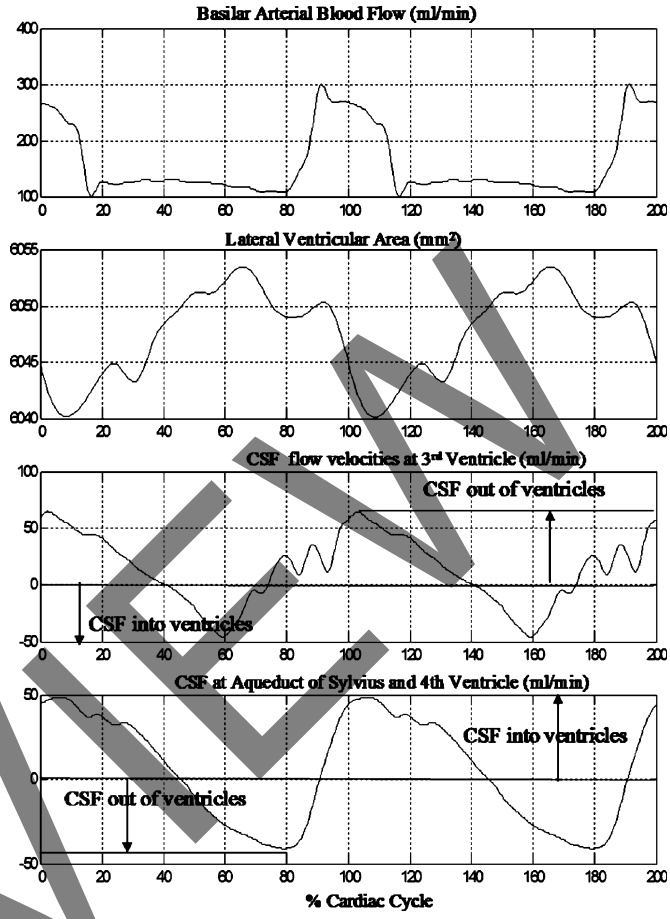

Fig. 1. Intracranial dynamics of an adult communicating hydrocephalus: The temporal relationship among the basilar artery, the lateral ventricle area, the CSF flow at the third ventricle and at the junction of the aqueduct of Sylvius and the fourth ventricle.

B. MRI Imaging and Image Reconstruction

T_1- and T_2-weighted images extracted from the MRI are introduced into *image reconstruction tools* [21]. Image reconstruction involves the physiologically accurate interpretation of the different substructures of the brain. Precise dimensions of the 3-D ventricular spaces, foramina and SAS are collected from 120 horizontally stacked MR slices of 1.5 mm spacing by connecting pixels of equal intensity delineating the boundaries

of the structures of interest. When connecting the 2-D information of each slice with the adjacent slices, a 3-D patient specific geometry of the brain or a subsection of it emerges.

After rendering surfaces which represent the boundaries between the parenchyma and the ventricular and SAS, Mimics image reconstruction software was used to further segment the 3-D volumes into a finite number of small triangular or tetrahedral elements [22]. This *triangulation* step is performed with a commercial grid generator tool Gambit. It partitions the patient-specific brain geometry information composed of volumes and boundary surfaces into a computational mesh with well-defined mathematical properties. Sagittal brain cuts are reconstructed for a 2-D analysis of the CSF flow.

C. Computational Analysis of MRI Flow Patterns

In order to interpret the experimental data and to understand the dynamic forces that cause CSF motion, a computational model for predicting the CSF fluid motion inside the cranial vault for each patient was designed. The CSF spaces inside the brain were extracted from the MR images and discretized versions of the mass and momentum balances were solved with computational fluid methods. Because the mathematical model only used these fundamental conservation laws of mass and momentum, it is referred to as a *first principles model*. Despite the large data set necessary to accurately represent the patients' brain geometry, the first principle fluid mechanics approach only requires a small number of physical parameters. The values of physical constants including the CSF viscosity (μ), density (ρ) as well as porosity (φ) and permeability (k) of the porous brain are listed in Table II. In addition, a set of boundary conditions needs to be specified. The results of the CSF analysis are the flow rate, velocities, and ICP gradients of CSF in the ventricular system as well as the porous parenchyma. The following discussion of the computational approach will introduce the mathematical equations, the boundary conditions as well as a subsection on the numerical solution of the large-scale partial differential equations.

1) CSF Flow in the Ventricular and Subarachnoid Systems: CSF motion is described by the equations of mass and momentum conservation for an incompressible Newtonian fluid [23]. These conservation balances lead to a system of partial differential equations known as the continuity and the Navier-Stokes equations. The governing equations for CSF flow are given in vector form by (1) and (2).

Conservation of mass

$$\vec{\nabla} \cdot \vec{q} = 0. \tag{1}$$

Conservation of momentum

$$\rho \left(\frac{\partial \vec{q}}{\partial t} + \vec{q} \cdot \vec{\nabla} \vec{q} \right) = -\vec{\nabla} p + \mu \, \vec{\nabla}^2 \vec{q} \tag{2}$$

where $\vec{q}$ is the velocity vector, ρ is the CSF density, and μ its viscosity.

CSF Flow Inside the Porous Brain Tissues: CSF is produced in the choroid plexus from the blood and also from the brain tissue from which it is believed to seep through the porous extracellular space towards the ventricles. Two thirds of the CSF production enters the ventricles from the choroid arteries [24], [25], one third is believed to be generated diffusely throughout the brain parenchyma. The CSF flow though the extracellular space of the brain parenchyma is modeled by a continuity equation and the momentum equation for flow though porous media. Accordingly, the continuity equation of CSF flow in the parenchyma has a source term S to account for new CSF production as in (3). The momentum balances of CSF seepage are the Navier-Stokes equations augmented by an additional term quantifying frictional interaction of CSF with the brain tissue. Here, $\vec{q}$ is the physical velocity vector flowing through the interstitial medium which is related to the superficial velocity through the extracellular volume fraction. Fluid flow through porous tissue experiences additional pressure drop proportional to the squared flow velocity through the porous tissue. Equation (4) is a generalization of the simpler Darcy's law of flow through porous media [26], [27]. In this paper, the brain tissue is treated as a homogeneous isotropic porous medium. The material properties, k, the permeability of the brain tissue, and β Forscheimer's coefficient measuring inertial resistance are listed in Table II. A more advanced physiologically consistent representation of the brain tissue would include anisotropy of the white matter leading to directional dependence of the permeability, porosity and diffusivities. These considerations are beyond the scope of this study.

CSF generation in the parenchyma

$$\vec{\nabla} \cdot \vec{q} = S. \tag{3}$$

CSF fluid seepage through the porous medium

$$\rho \left(\frac{\partial \vec{q}}{\partial t} + \vec{q} \cdot \vec{\nabla} \vec{q} \right) = -\vec{\nabla} p + \mu \, \vec{\nabla}^2 \vec{q} - \left(\frac{\mu}{k} \vec{q} + \frac{\beta \rho}{2} \vec{q}^2 \right). \tag{4}$$

Boundary Conditions for Intracranial Dynamics: Fig. 2 illustrates the location of the boundaries within a 2-D sagittal cut of a normal subject. The boundary conditions for the CSF flow in the cranium are summarized in Table I. The bulk production is due to CSF generation in the choroid plexus and parenchyma. The diffuse production of CSF flow throughout the parenchyma is accounted for as a source term introduced in (3). The bulk CSF production is implemented as input flux at the choroid plexus.

Recently, we have shown that the expansion of the vascular bed in the systole leads to compression of the lateral ventricle as well as enlargement of the choroid plexus resulting in CSF flow out of the ventricles [20]. For this study, the action of the vascular expansion bed is accounted for via the boundary condition for the choroid plexus as given by (5). Thus, the choroid boundary condition accounts for the constant CSF production as well as the pulsatile flow of CSF due to expansion of the parenchyma as well as choroid plexus in the systole [8], [28]. The frequency of the pulsatile motion is set to 1 Hz approximating the normal cardiac cycle.

Most scientists believe that the majority of reabsorption of the CSF is into the granulation of the sagittal sinuses. Accordingly, re-absorption of the fluid takes place at the top of the brain geometry. The re-absorption is assumed to be proportional to the pressure difference between the ICP in the SAS and the venous pressure inside the sagittal sinus [29]. This relation is expressed mathematically by (6).

The expansion of the vascular bed also causes displacement of CSF from the cranium into the spinal SAS. The fluid displace-